Construction and Building Materials 26 (2012) 216–225

Contents lists available at ScienceDirect

Construction and Building Materials

journal homepage: www.elsevier.com/locate/conbuildmat

Splice strength of large diameter, high strength steel reinforcing bars

Tarek K. Hassan [a,*], Gregory W. Lucier [b], Sami H. Rizkalla [b]

[a] Structural Engineering Department, Faculty of Eng., Ain Shams University, Cairo, Egypt
[b] Department of Civil, Construction and Environmental Engineering, NCSU, Raleigh, NC, USA

ARTICLE INFO

Article history:
Received 5 January 2011
Received in revised form 30 April 2011
Accepted 13 June 2011
Available online 8 July 2011

Keywords:
Beams
Bond
Concrete
Confinement
Development length
High strength reinforcement
Splice strength

ABSTRACT

The results of an experimental program conducted to study the splice strength of large diameter, high strength reinforcing bars, either No. 20 (63.5 mm diameter) or No. 9 (28 mm diameter), are presented. The parameters included in the experimental program are the bar size, splice length, concrete compressive strength, and the amount of transverse reinforcement provided within the splice zone. The ability of several models including the current ACI 318 Building Code, to predict the maximum steel stresses at the onset of splitting failure was examined for these high strength, large diameter bars. The influence of the moment of inertia of the bar on the induced splitting stresses was evaluated numerically using finite element analysis. Test results showed that the presence of transverse reinforcement has a more pronounced effect for large diameter spliced-bars compared to regular size bars. It is also shown that the current ACI 318 Building Code provided more conservative bond strength predictions for regular bars compared to large diameter bars.

1. Introduction

The main parameters that influence the bond strength of steel reinforcing bars embedded in concrete are well documented in the literature. These parameters include concrete cover, bar spacing, bar casting position, development/splice length, bar size and geometry, bar surface condition, yield strength of bars, concrete compressive and tensile strength, aggregate type and quantity, concrete slump and workability admixtures, and the amount of transverse reinforcement provided in the splice or development region [1–10]. One of the earliest and most valuable studies on bond behavior of reinforcing bars was conducted by Orangun et al. [2]. Based on regression analysis of 62 unconfined concrete specimens and 54 confined concrete specimens, a simplified general design expression for the maximum measured steel stress in the spliced bars, f_s at the onset of splitting failure was developed as given in the following equation:

$$\frac{A_b f_s}{\sqrt{f'_c}} = 3\pi l_d(c_{\min}+0.4d_b)+200A_b+\frac{\pi l_d A_{tr} f_{yt}}{500sn} \quad \text{Units are in lb and in.}$$
$$\frac{A_b f_s}{\sqrt{f'_c}} = 0.25\pi l_d(c_{\min}+0.4d_b)+16.6A_b+\frac{\pi l_d A_{tr} f_{yt}}{41.5sn} \quad \text{Units are in N and mm} \tag{1}$$

Based on the work of Darwin et al. [3,4], ACI Committee 408 developed more refined design provisions for spliced bars as expressed in the following equation:

$$\frac{A_b f_s}{\sqrt[4]{f'_c}} = [59.9l_d(c_{\min}+0.5d_b)+2400A_b]\left(0.1\frac{c_{\max}}{c_{\min}}+0.9\right)+\left(30.88t_r t_d\frac{NA_{tr}}{n}+3\right)\sqrt{f'_c} \quad \text{Units are in lb and in.}$$
$$\frac{A_b f_s}{\sqrt[4]{f'_c}} = [1.43l_d(c_{\min}+0.5d_b)+57.4A_b]\left(0.1\frac{c_{\max}}{c_{\min}}+0.9\right)+\left(8.9t_r t_d\frac{NA_{tr}}{n}+558\right)\sqrt{f'_c} \quad \text{Units are in N and mm} \tag{2}$$

Despite the extensive data base used in developing these provisions, most of the data were obtained from tests of embedded bars having diameters less than No. 11 (35 mm) and specified yield strengths less than 80 ksi (550 MPa). It should be noted that the current ACI 318-08 [11] provisions for development and splice strength are empirical and are based primarily on the expression developed by Orangun et al. [2]. In these provisions, it is prohibited to use lap splices for reinforcing bars larger than No. 11 (35 mm diameter). Lack of test data on the bond strength of large diameter deformed steel bars is the primary reason for the current limit included in the ACI 318 Building Code.

In an attempt to evaluate the validity of this limitation, an experimental program was undertaken at the Constructed Facilities Laboratory at North Carolina State University to evaluate the

* Corresponding author. Address: 14 Gamal Nouh Street, Almaza, Heliopolis, Cairo, Egypt. Tel.: +20 2010 2188906.
E-mail address: tarek.hassan@dargroup.com (T.K. Hassan).

0950-0618/$ - see front matter © 2011 Elsevier Ltd. All rights reserved.
doi:10.1016/j.conbuildmat.2011.06.013

Nomenclature

A_b	area of bar being developed or spliced	f_y	yield strength of steel being spliced
A_{str}	area of one leg of stirrups at the splice region	f_{yt}	yield strength of transverse reinforcement
A_{tr}	area of each stirrup crossing the potential plane of splitting adjacent to the reinforcement being spliced	l_d	development length
		l_s	splice length
c_t	top concrete cover for reinforcing bar being spliced	n	number of bars being spliced
c_{max}	maximum (c_t, c_s)	N	number of transverse stirrups within the splice length
c_{min}	minimum (c_t, c_s)	R_r	relative rib area of the reinforcement
c_s	minimum [c_{so}, c_{si} + 0.25 in. (6.35 mm)]	s	spacing of transverse reinforcement
c_{si}	1/2 of the bar clear spacing	t_d	term representing the effect of bar size = $0.72d_b + 0.28$, ($0.028d_b + 0.28$)
c_{so}	side concrete cover for reinforcing bar		
d_b	diameter of bar	t_r	term representing the effect of relative rib area = $9.6R_r + 0.28$
f'_c	concrete compressive strength		
f_s	stress in reinforcing bar	u	bond stress

splice strength of No. 20 (63.5 mm diameter) bars compared to that of No. 9 (28 mm diameter) bars. A total of 20 full-scale reinforced concrete beams were constructed and tested. The beams were reinforced with high-strength steel bars spliced within the constant moment region. The ability of current code provisions to predict the splice strength is examined. The influence of the splice length, confinement level, and bar moment of inertia on the induced splitting stresses is discussed.

This study provides unique data on the bond behavior of large diameter high-strength steel reinforcing bars using 48 ft (14.6 m) long concrete beams complementing earlier studies using small scale specimens. The experimental results presented herein, along with the analytical investigation and comparison with previous studies are useful for better understanding of the bond characteristics and for investigating the influence of confinement on large diameter steel bars. The knowledge gained from this study is significant for the assessment of code provisions for large diameter bars in order to have these bars generally accepted and used in practice.

2. Experimental investigation

2.1. Test specimens

The test program consisted of 20 full-scale beam specimens with spliced tensile reinforcement at mid-span. The beams were divided into five main groups. Each group was comprised of four specimens having similar concrete compressive strength. The first beam in each group did not contain any transverse reinforcement within the splice zone. The second and third beams in each group were identical and were confined with transverse reinforcement within the splice zone. The fourth beam in each group contained double the transverse reinforcement used in the second and third beams. All beams were tested under four point bending to provide a constant moment region at the location of the splice. Groups 1, 2 and 3 consisted of 12 concrete beams, each reinforced with three No. 9 (28 mm diameter) bars, placed at the tension side of the beam and spliced at mid-span. The beams were 22 ft (6.7 m) long and had a rectangular cross section of 16 in. wide × 20 in. deep (406 mm × 508 mm). Two No. 4 (13 mm diameter) bars were placed longitudinally in the compression region of the beam to minimize cracking during transportation and to hold the beam together after rupture of the splice. The beams were reinforced with No. 3 (10 mm diameter) stirrups spaced every 9 in. (230 mm) outside the splice region to prevent shear failure. Groups 4 and 5 were comprised of eight concrete beams, each reinforced with two No. 20 (63.5 mm diameter) bars, placed in the tension side of the beam and spliced at mid-span. The beams were 48 ft (14.6 m) long and had a rectangular cross section of 18 in. wide × 30 in. deep (457 mm × 762 mm). Four No. 11 (35 mm diameter) bars were placed longitudinally in the compression region of the beam. The beams were reinforced with No. 5 (16 mm diameter) stirrups spaced every 6 in. (152 mm) outside the splice region to prevent shear failure. Fig. 1 shows the reinforcement details of the splice beams tested in this program. The splice lengths for the beams in groups 1, 2, 4 and 5, were designed according to the ACI 318 Building Code to achieve the yield strength of the steel bars. In order to examine the ability of the code provisions to predict the splice strength prior to yielding of the bars, the splice lengths for the concrete beams in group 3 were selected to achieve half of the yield strength of the bars. Design was performed using nominal concrete compressive strength of 6000 psi (41 MPa) for groups 1, 3, and 4 whereas for groups 2 and 5 a concrete compressive strength of 12,000 psi (82 MPa) was used to complement the high tensile strength of the reinforcing bars. Table 1 provides a summary of the specimens' designation and test parameters.

2.2. Test setup and instrumentation

The beams were tested under four point bending in an inverted position to allow observation and monitoring of the cracks on the top surface of the beam. For all beams, electrical resistance strain gauges were attached to the top of the steel bars approximately 1 in. (25 mm) away from the end of the splice length to monitor the strains developed in the bars. In addition, PI gauges were mounted on the compression face of the specimen to monitor strains in the compression zone. Five string potentiometers were attached to the bottom face of the specimen at the location of the supports, at quarter points, and at the center of the beam to monitor deflections. The test setup for the concrete specimens tested in groups 1, 2, and 3 included two 135 kips (600 kN) calibrated hydraulic jacks located at the quarter-spans of each beam while four 135 kips (600 kN) jacks were used to achieve the higher loads required for testing the concrete specimens in groups 4 and 5. Two steel crossbeams were used to tie the ends of each specimen to the testing floor. A steel plate was placed on a leveled pad of non-shrink grout at the end of each specimen, directly underneath the tie-down beams. Calibrated load cells were placed on top of the steel plates and underneath the tie down beams. Fig. 2 and 3 show schematic and photographs of the test setup for splice beams in different groups.

2.3. Materials

2.3.1. Reinforcing steel

The spliced reinforcing bars, No. 9 (28 mm diameter) and No. 20 (63.5 mm diameter) were threaded over their entire length. The tensile stress–strain behavior of the bars is shown in Fig. 4. The bars have an elastic modulus of elasticity of 29,000 ksi (200 GPa). According to the ASTM A370-07 [12] offset method (0.2% offset), the yield strength of the bars ranged from 106 to 109 ksi (730–750 MPa). The ultimate tensile strength of the bars ranged from 124 to 132 ksi (855–910 MPa). The relative rib areas of No. 9 (28 mm diameter) and No. 20 (63.5 mm diameter) bars were 0.18 and 0.16, respectively. Other reinforcing bars used in the test program were Grade 60 deformed bars. The bars have a yield strength of 60 ksi (414 MPa) and modulus of elasticity of 29,000 ksi (200 GPa).

2.3.2. Concrete

A commercial ready mix plant supplied the concrete. Two different concrete mixtures were designed to achieve a 6000 psi (41 MPa) and 12,000 psi (82 MPa) concrete. Portland cement, washed sand, and aggregate of 0.75 in. (19 mm) maximum size were used to prepare the low strength concrete mixture. A super plasticizer was added to the second mixture to achieve the high strength concrete. The maximum aggregate size in the second mixture was 3/8 in. (10 mm). The compressive strength of concrete was determined at the day of testing the splice beams using 4 × 8 in. (102 × 204 mm) cylinders cast at the same time as the specimens and cured alongside the specimens. The concrete compressive strength of the test specimens is given in Table 1.

3. Experimental results

3.1. General behavior and mode of failure

During the early stage of load application, flexural cracks initiated in the constant moment zone just outside the splice region.

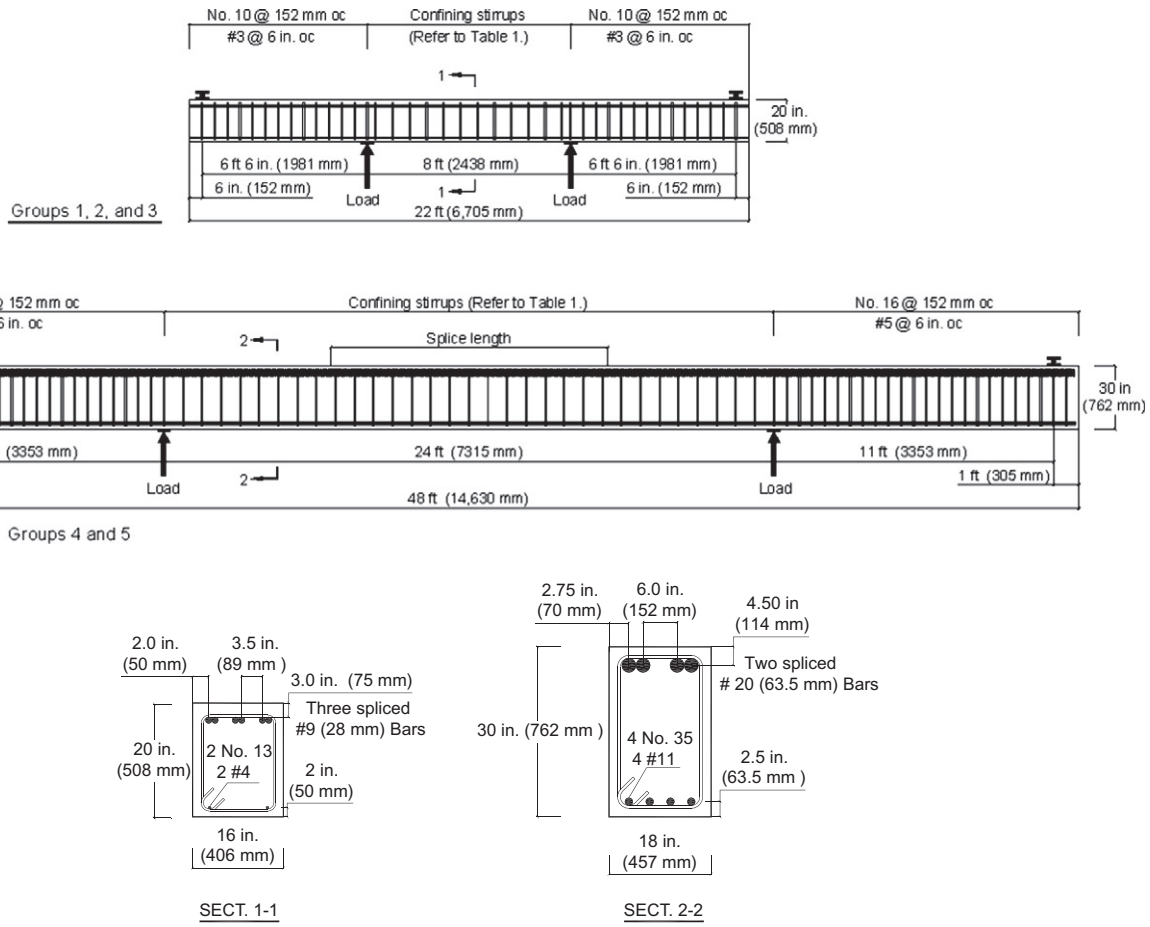

Fig. 1. Reinforcement details of splice beam specimens.

Table 1
Properties of splice beam specimens.

Group	Specimen	d_b (in.)	n	l_s (in.)	R_r	f'_c (psi)	c_t (in.)	c_{so} (in.)	c_{si} (in.)	c_s (in.)	c_{min} (in.)	N	A_{str} (in.) [2]	f_s (ksi)	f_s/f_y
1	B1.1	1.125	3	64	0.18	6300	3.0	1.44	1.19	1.44	1.44	0	0.00	104	0.95
	B1.2	1.125	3	60	0.18	6300	3.0	1.44	1.19	1.44	1.44	3	0.11	95	0.87
	B1.3	1.125	3	60	0.18	6300	3.0	1.44	1.19	1.44	1.44	3	0.11	95	0.87
	B1.4	1.125	3	56	0.18	6300	3.0	1.44	1.19	1.44	1.44	8	0.11	93	0.85
2	B2.1	1.125	3	46	0.18	9400	3.0	1.44	1.19	1.44	1.44	0	0.00	110	1.01
	B2.2	1.125	3	43	0.18	10,100	3.0	1.44	1.19	1.44	1.44	3	0.11	111	1.01
	B2.3	1.125	3	43	0.18	10,100	3.0	1.44	1.19	1.44	1.44	3	0.11	112	1.02
	B2.4	1.125	3	40	0.18	9400	3.0	1.44	1.19	1.44	1.44	6	0.11	112	1.02
3	B3.1	1.125	3	32	0.18	7460	3.0	1.44	1.19	1.44	1.44	0	0.00	59	0.54
	B3.2	1.125	3	30	0.18	7460	3.0	1.44	1.19	1.44	1.44	3	0.11	59	0.54
	B3.3	1.125	3	30	0.18	7460	3.0	1.44	1.19	1.44	1.44	3	0.11	59	0.54
	B3.4	1.125	3	28	0.18	7460	3.0	1.44	1.19	1.44	1.44	4	0.11	58	0.53
4	B4.1	2.50	2	235	0.16	6000	3.25	1.5	1.75	1.5	1.5	0	0.00	83	0.78
	B4.2	2.50	2	207	0.16	6000	3.25	1.5	1.75	1.5	1.5	12	0.20	105	0.99
	B4.3	2.50	2	207	0.16	7700	3.25	1.5	1.75	1.5	1.5	12	0.20	105	0.99
	B4.4	2.50	2	185	0.16	8400	3.25	1.5	1.75	1.5	1.5	21	0.20	107	1.00
5	B5.1	2.50	2	166	0.16	11,300	3.25	1.5	1.75	1.5	1.5	0	0.00	85	0.80
	B5.2	2.50	2	146	0.16	11,100	3.25	1.5	1.75	1.5	1.5	8	0.20	98	0.92
	B5.3	2.50	2	146	0.16	10,300	3.25	1.5	1.75	1.5	1.5	8	0.20	93	0.88
	B5.4	2.50	2	131	0.16	10,100	3.25	1.5	1.75	1.5	1.5	15	0.20	107	1.00

Note: 1 in. = 25.4 mm, 1000 psi = 1 ksi = 6.895 MPa.

As the load increased, flexural cracks propagated randomly along 75–100% of the splice length at ultimate load. At approximately 50% of the ultimate load, splitting cracks formed simultaneously at both ends of the splice and propagated towards mid-span. Additional splitting cracks were also observed and initiated from the existing transverse flexural cracks at the top surface of the beam specimens below the reinforcing bars. As the load increased, the side and top splitting cracks propagated along the full length of

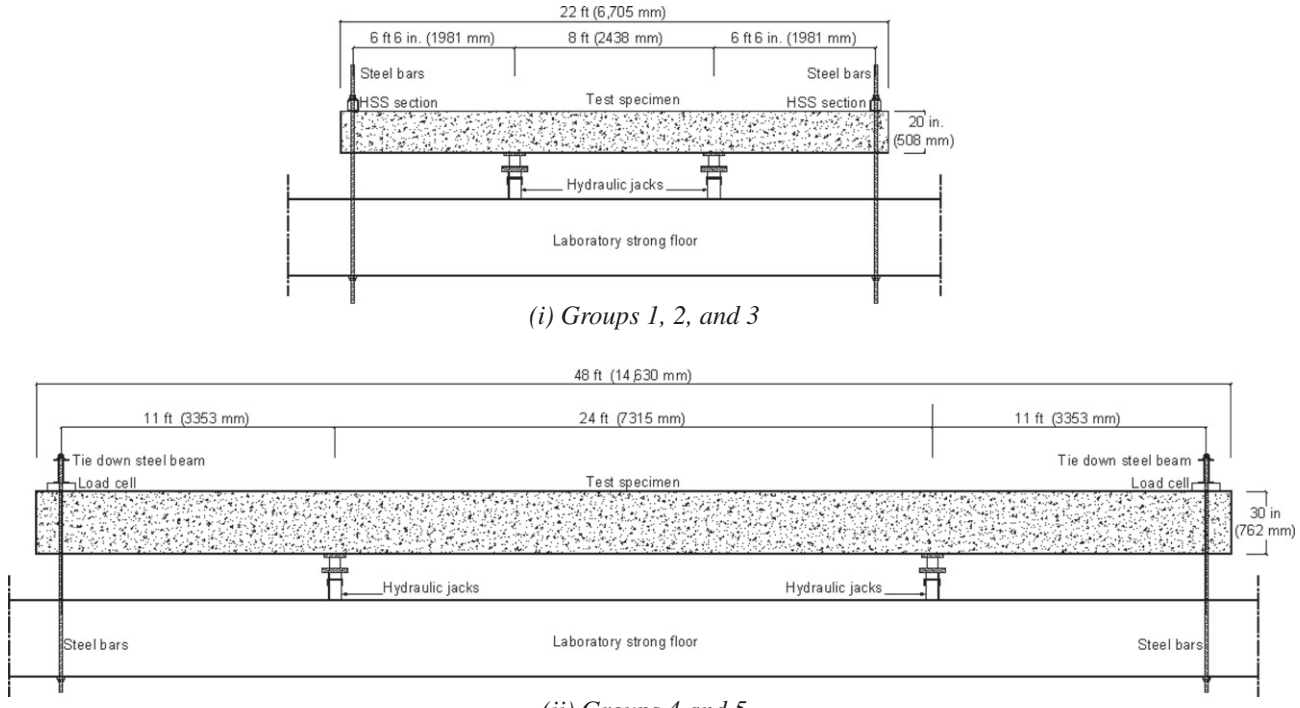

Fig. 2. Schematic of test set-up for splice beams.

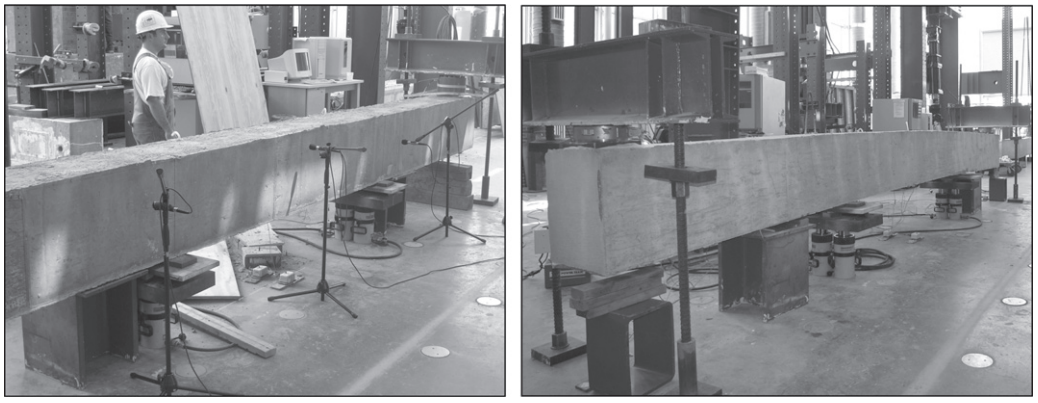

(i) Groups 1, 2, and 3 *(ii) Groups 4 and 5*

Fig. 3. Splice beams prior to testing.

the spliced bars in a clear and well defined pattern. Side splitting of the concrete cover was the prevailing mode of failure for all the tested specimens. It should be noted that the top cover in all the specimens was significantly larger than half of the clear spacing between the spliced bars. Therefore, side splitting failure was clearly the dominant failure mode of all the tested specimens. For the unconfined concrete specimens, failure was sudden, violent and complete along the splice length as shown in Fig. 5a and b for concrete beams reinforced with No. 9 (28 mm diameter) and No. 20 (63.5 mm diameter) bars, respectively. Failure was accompanied by a complete loss in load resistance and a sudden drop of the applied load. Confined concrete specimens exhibited a more ductile post-splitting behavior. Nevertheless, the failure was also brittle as demonstrated in Fig. 6a and b. The transverse reinforcements within the splice region were unable to confine the failure nor reduce spalling of the concrete specially for the No. 20 (63.5 mm diameter) bars. This behavior could be attributed to the large moment of inertia of the bars, which induced additional splitting stresses as will be discussed in the following sections.

3.2. Developed stresses

Figs. 7a–e depict the applied moment versus the maximum measured steel stress normalized to $f_c'^{0.5}$ for the different beam groups. The figure indicates identical behavior for the concrete beams reinforced with No. 9 (28 mm diameter) bars in groups 1, 2 and 3 as shown in Fig. 7a–c, respectively. It should be noted that the concrete beams within each group were designed according to the ACI 318 Building Code to achieve the same splice strength. Such a criterion was accomplished by varying the splice length from one beam to the other depending on the confinement level provided within the splice region. Therefore, this identical behavior was expected for regular diameter reinforcing bars and indicates that the influence of the confining transverse reinforcement within

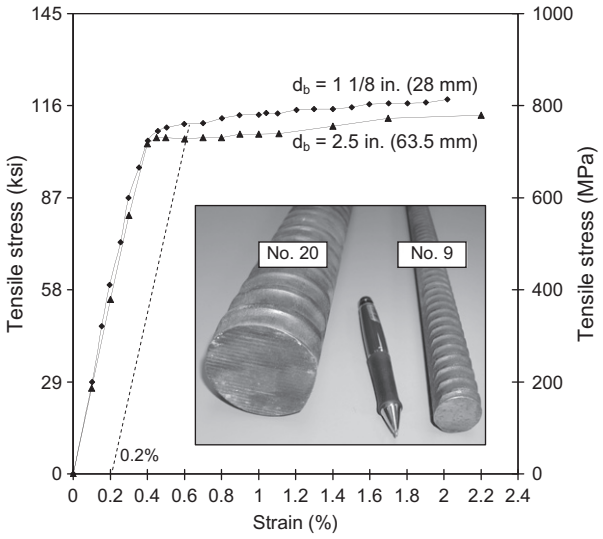

Fig. 4. Stress–strain characteristics of high strength steel.

the splice region is well accounted for in the code provisions. Conversely, a significant discrepancy was observed among the concrete beams reinforced with No. 20 (63.5 mm diameter) bars in groups 4 and 5 as shown in Fig. 7d and e, respectively. At any applied moment, the normalized measured tensile stresses were much higher in the unconfined specimen compared to the confined specimen as shown in Fig. 7d. This behavior was highly pronounced in concrete beams having lower concrete compressive strength. The observed behavior strongly demonstrates the greater influence of the confining transverse reinforcement on the splice strength of large diameter bars compared to regular diameter bars. Test results showed also that it is not possible to develop the yield strength of No. 20 (63.5 mm diameter) bars without the use of transverse reinforcement confining the splice region. In order to further enumerate the effect of transverse reinforcement, the average normalized bond strength, $u/f_c'^{0.5}$, is plotted versus $A_{tr}f_{yt}/(snd_b)$ as shown in Fig. 8. The parameter $A_{tr}f_{yt}$ represents the force, which can be developed in the transverse reinforcement crossing the potential plane of splitting. The average bond stress, u, was determined based on the force developed in the bar at ultimate load and the surface area of the bar along the splice length as given by the following equation:

$$u = \frac{A_b f_s}{\pi d_b l_s} \tag{3}$$

Fig. 8 clearly shows that increasing the transverse restraint relative to bar diameter increases the normalized bond strength in addition to that provided by the concrete cover alone. Such an effect is more perceptible for the concrete beams reinforced with No. 20 (63.5 mm diameter) bars as reflected by the flatter slope of the best fitting line passing through the test results for the concrete beams reinforced with No. 9 (28 mm diameter) bars compared to those reinforced with No. 20 (63.5 mm diameter) bars.

4. Comparison with code and empirical design expressions

The maximum measured steel stresses at the onset of splitting failure for all tested beams were compared to those calculated

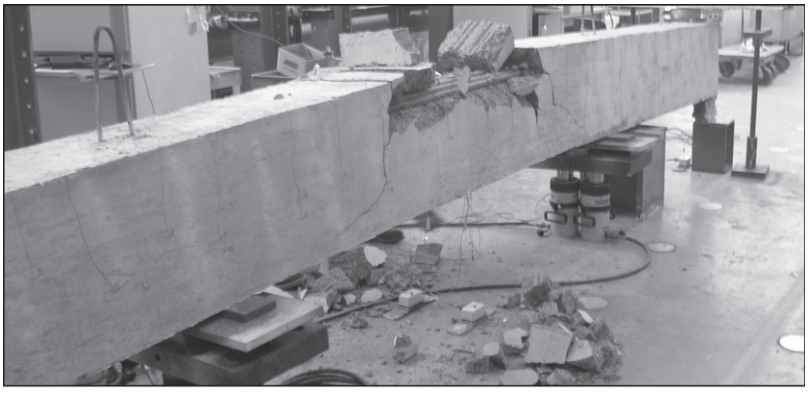

(a) Beams reinforced with No. 9 (28 mm diameter) bars

(b) Beams reinforced with No. 20 (63.5 mm diameter) bars

Fig. 5. Typical side splitting failure for unconfined concrete beams.

(a) Beams reinforced with No. 9 (28 mm diameter) bars

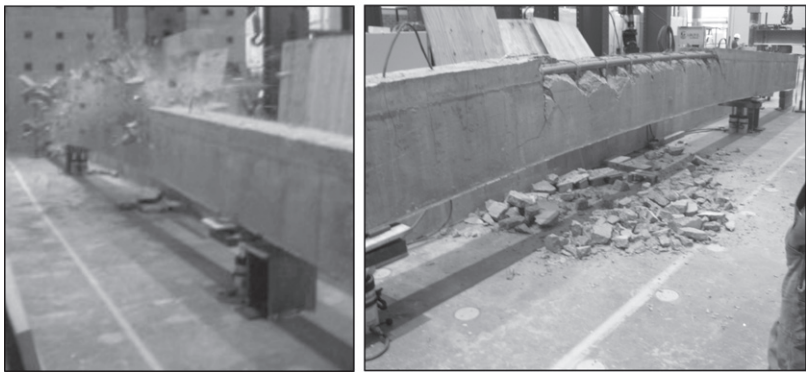

(b) Beams reinforced with No. 20 (63.5 mm diameter) bars

Fig. 6. Typical side splitting failure for confined concrete beams.

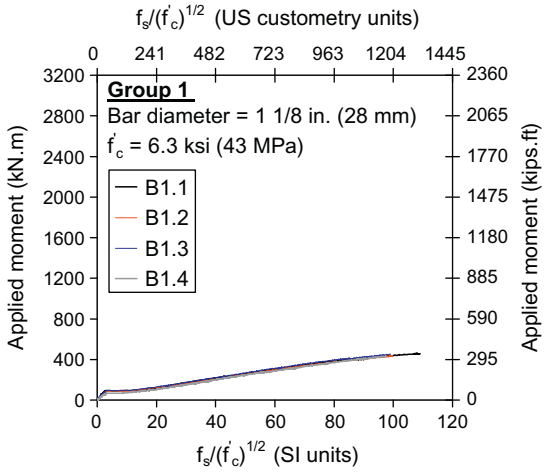

Fig. 7a. Applied moment versus normalized steel stress for group 1 beams.

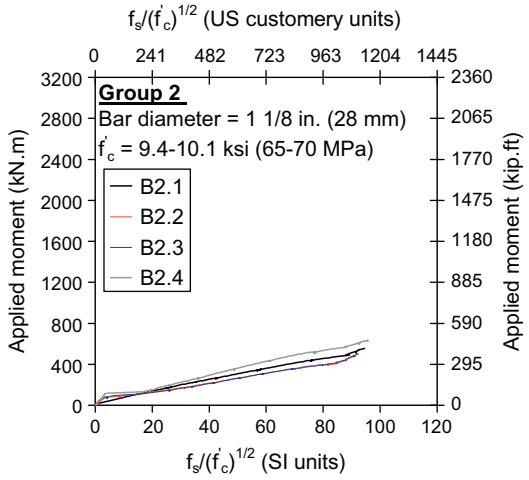

Fig. 7b. Applied moment versus normalized steel stress for group 2 beams.

using the well known expressions proposed by Orangun et al. [2], (Eq. (1)), ACI Committee 408 [1] (Eq. (2)) and ACI 318-08 [11] design provisions. The development length l_d in these expressions was replaced by $l_s/1.3$ to account for the bar casting position, where l_s is the splice length. Fig. 9a and b show that the predicted steel stresses versus the measured values for the unconfined and confined concrete beams reinforced with No. 9 (28 mm diameter) bars using different design expressions. In general, the predicted stresses using any of the three approaches were in good agreement with the measured values. The beneficial effect of confinement on the splice strength of these beams is represented with sufficient accuracy in the three approaches. The average of the developed/predicted steel stress for the concrete beams reinforced with No. 9 (28 mm diameter) bars using ACI 318-08 is 1.25 with a standard deviation of 0.14.

The predicted versus the measured steel stresses for the unconfined and confined concrete beams reinforced with No. 20 (63.5 mm diameter) bars using different design expressions are shown in Fig. 10a and b. The ACI Committee 408 design expression predicted consistently higher stresses compared to the measured values specially for the confined specimens. This could be attributed to the large relative rib area of these bars, which exceeded

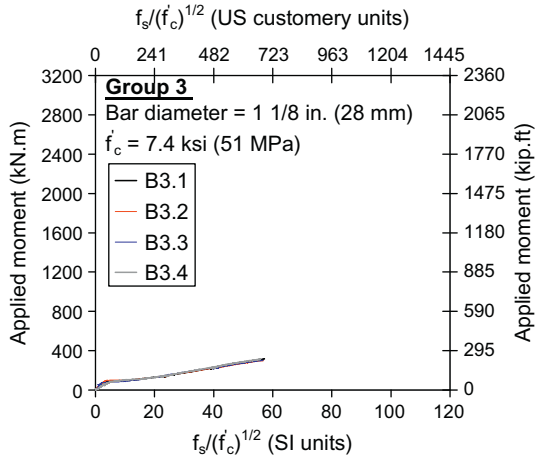

Fig. 7c. Applied moment versus normalized steel stress for group 3 beams.

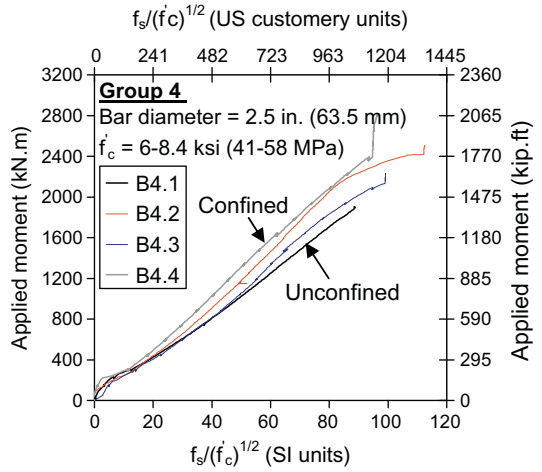

Fig. 7d. Applied moment versus normalized steel stress for group 4 beams.

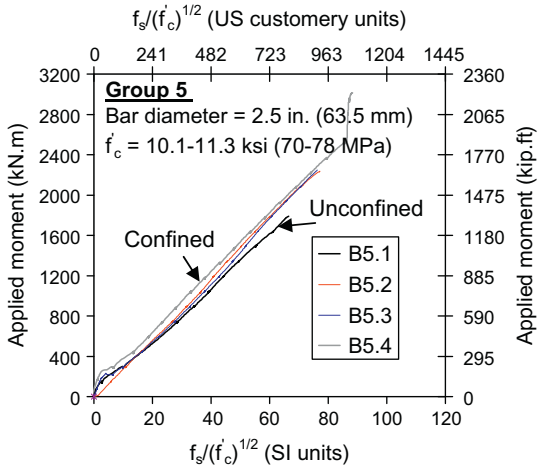

Fig. 7e. Applied moment versus normalized steel stress for group 5 beams.

the values used in calibrating the ACI Committee 408 design expression. Although the predicted stresses using Orangun et al. [2], (Eq. (1)) and ACI 318-08 [11] design expressions are deemed satisfactory compared to the measured values, it is interesting to note that the safety margin is reduced considerably when using

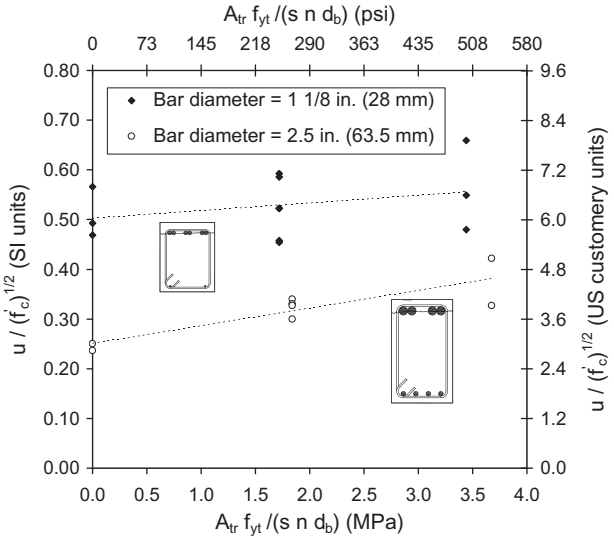

Fig. 8. Influence of transverse reinforcement.

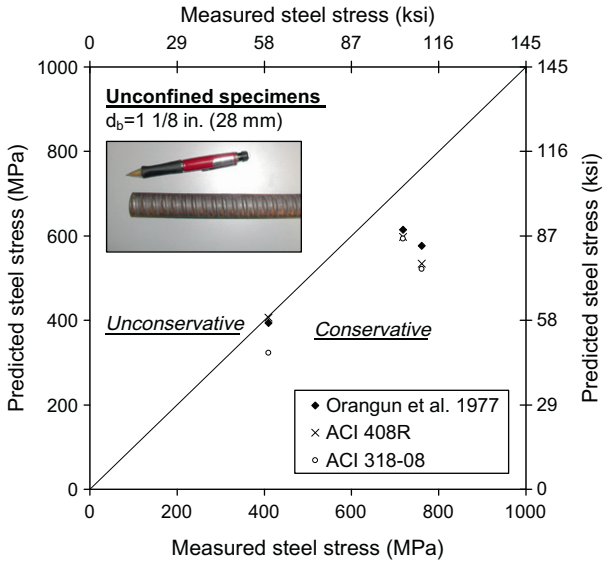

Fig. 9a. Predicted steel stresses versus the measured values using different approaches for the unconfined beams reinforced with No. 9 (28 mm diameter) bars.

these expressions to predict the developed stresses in No. 20 (63.5 mm diameter) bars particularly for the unconfined specimens. Such an observed trend suggests presence of additional splitting stresses around the large diameter bars and necessitates further analysis as will be discussed in the following section. The increase in splitting stresses could be attributed to the large moment of inertia of the bars with respect to the surrounding concrete. The average of the developed/predicted steel stress for the concrete beams reinforced with No. 20 (63.5 mm diameter) bars using ACI 318-08 is 1.15 with a standard deviation of 0.12. A summary of the developed and predicted steel stresses using different approaches is given in Table 2.

5. Analytical investigation

In an attempt to investigate the influence of the moment of inertia of large diameter bars on the induced splitting stresses, a

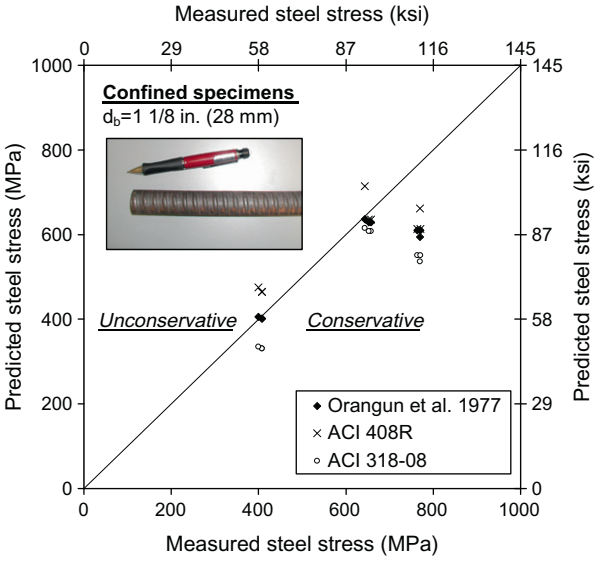

Fig. 9b. Predicted steel stresses versus the measured values using different approaches for the confined beams reinforced with No. 9 (28 mm diameter) bars.

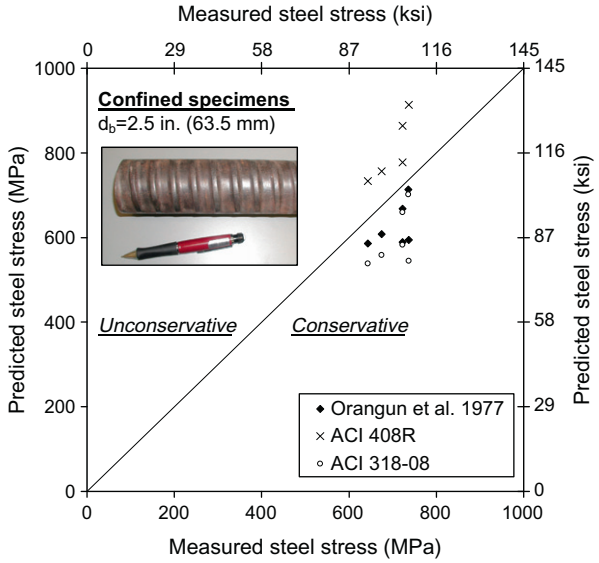

Fig. 10b. Predicted steel stresses versus the measured values using different approaches for the confined beams reinforced with No. 20 (63.5 mm diameter) bars.

non-linear finite element analysis was conducted using ANATECH Concrete Analysis Program (ANACAP) [13,14]. The concrete material model in ANACAP has evolved over the past 35 years and is based on the smeared cracking methodology. The compressive behavior of the concrete follows the generally accepted principles of computational plasticity. Within the concrete constitutive model, cracking and all other forms of material non-linearity are treated at the finite element integration points. Cracks are assumed to form perpendicular to the principal tensile strain direction in which the cracking criterion is exceeded. When cracking occurs, the stress normal to the crack direction is reduced to zero, which results in redistribution of stresses around the crack. The ability of cracked concrete to share the tensile forces with the steel reinforcement between cracks is modeled in ANACAP by means of a tension softening model. The modeling of concrete also includes residual tension stiffness for the gradual transfer of load to the reinforcement during crack formation. The program also accounts for the reduction in shear stiffness due to cracking and further

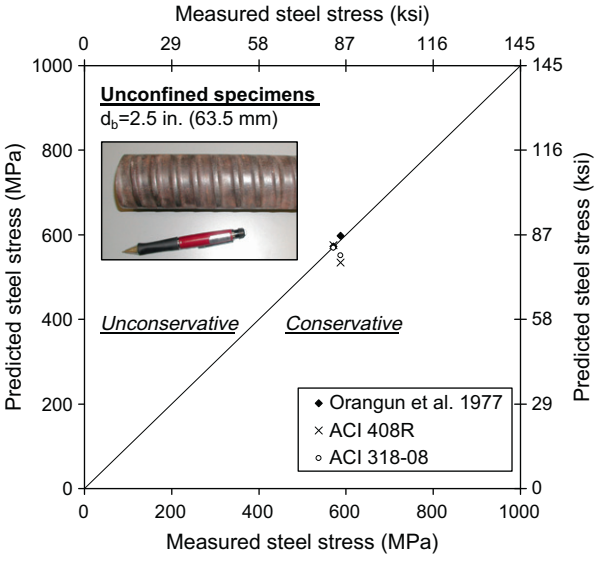

Fig. 10a. Predicted steel stresses versus the measured values using different approaches for the unconfined beams reinforced with No. 20 (63.5 mm diameter) bars.

Table 2
Comparison between measured and predicted steel stresses.

Group	Specimen	Measured/predicted steel stress		
		Orangun et al. 1977	ACI 408R	ACI 318-08
1	B1.1	1.17	1.20	1.21
	B1.2	1.04	1.03	1.08
	B1.3	1.04	1.03	1.07
	B1.4	1.01	0.90	1.05
2	B2.1	1.32	1.42	1.46
	B2.2	1.25	1.24	1.38
	B2.3	1.26	1.26	1.40
	B2.4	1.30	1.16	1.43
3	B3.1	1.04	1.01	1.27
	B3.2	1.02	0.88	1.23
	B3.3	1.02	0.88	1.23
	B3.4	0.99	0.84	1.20
Mean		1.12	1.07	1.25
Standard deviation		0.13	0.19	0.14
4	B4.1	1.00	0.99	1.00
	B4.2	1.23	0.93	1.24
	B4.3	1.08	0.84	1.10
	B4.4	1.03	0.67	1.05
5	B5.1	0.98	1.10	1.06
	B5.2	1.11	0.89	1.21
	B5.3	1.10	0.88	1.20
	B5.4	1.24	0.81	1.35
Mean		1.10	0.89	1.15
Standard deviation		0.10	0.13	0.12

decay as the crack opens. The reinforcement is modeled as individual sub-elements within the concrete elements. Rebar sub-element stiffnesses are superimposed on the concrete element stiffness in which the rebar resides. More details and validation of the program using independent test results can be found elsewhere [15–17]. Taking advantage of the symmetry in geometry and loading conditions, half of the concrete specimen B4.3, reinforced with No. 20 (63.5 mm diameter) bars was modeled using 20-node brick elements. Each node has three translational degrees of freedom. The finite element mesh was chosen so that elements would maintain an acceptable aspect ratio. The spliced reinforcements were modeled as truss elements embedded in the concrete elements.

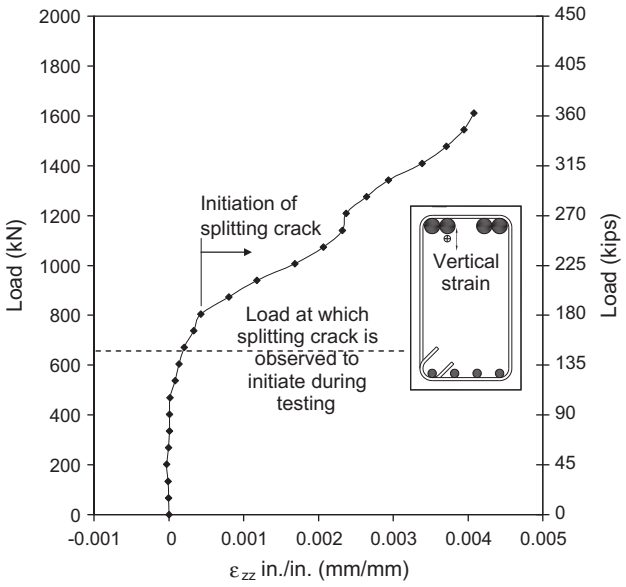

Fig. 11. Predicted transverse strains at the bar cutoff point.

The applied load versus the transverse strain at the spliced bar cutoff location is shown in Fig. 11. Results of the analysis showed that initiation of splitting cracks were predicted at a load level of 180 kips (800 kN), which is 20% higher than the measured value. Such a difference between the predicted and measured values is expected to take place as a result of the assumed numerical modeling parameters for the concrete properties, boundary conditions, mesh size and loading steps. In the model, formation of splitting cracks is accompanied by a significant increase in the strain with slight increase in load. Initial trials to use solid elements to model the spliced reinforcement provided significant restraints to formation of splitting cracks due to the full bond between the bars and the concrete as assumed by the program in the transverse direction. Modeling of the reinforcement as beam elements was also not possible in ANACAP due to the difference in the degrees of freedom at the connecting nodes. In order to investigate the influence of bar diameter on the induced splitting stresses after concrete cracking, the analysis was performed using SAP2000 [18] in which the beam was modeled using 8-node solid elements and the reinforcements were modeled using either beam or truss elements. The analysis assumed a reduced modulus of elasticity for the middle portion of the beam to account for cracking as shown in Fig. 12. The resulting transverse stress contours at the end of the bar cutoff point is shown in Fig. 13a and b using truss and beam elements, respectively. Localized tensile stress contours around the spliced bar were predicted in the analysis demonstrating the tendency of the bar to straighten out as the beam deforms. Results of the analyses showed that the induced splitting stresses increased by 15% when using beam elements and accounting for the moment of inertia of the bars compared to those predicted using truss elements. The analysis shows pronounced increase in splitting stresses for beams without transverse reinforcement within the splice region. The analysis depicts an increase of 25% in splitting stresses using beam elements compared to those predicted using truss

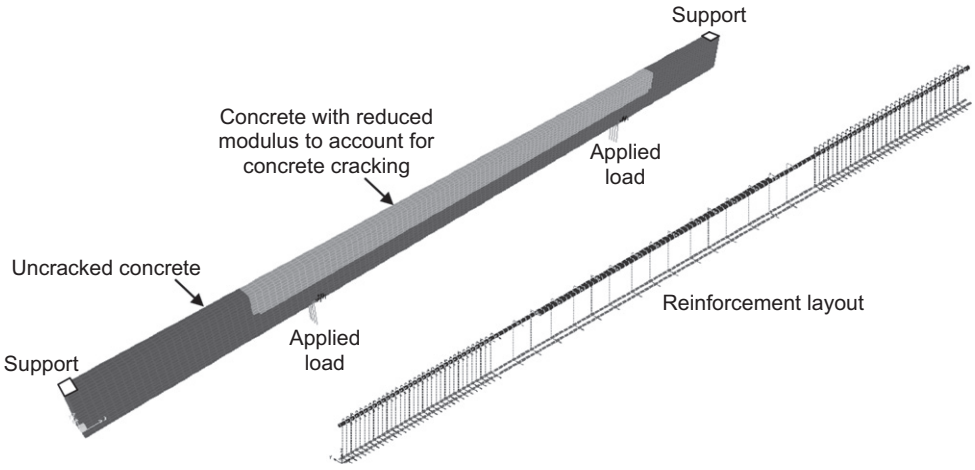

Fig. 12. Finite element model used in analysis.

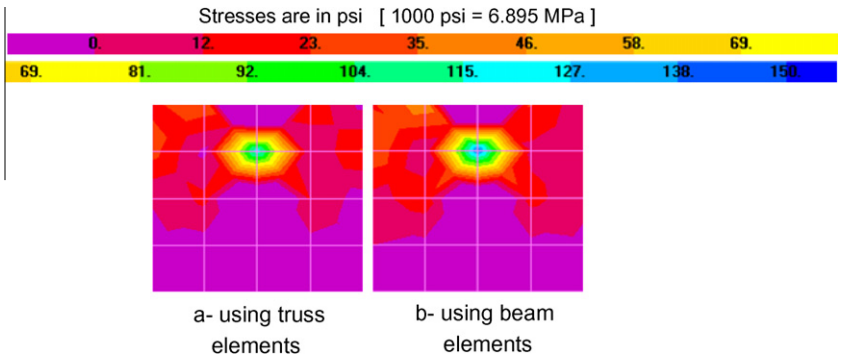

Fig. 13. Stress contours at the spliced bar cutoff point with transverse reinforcement in the splice region.

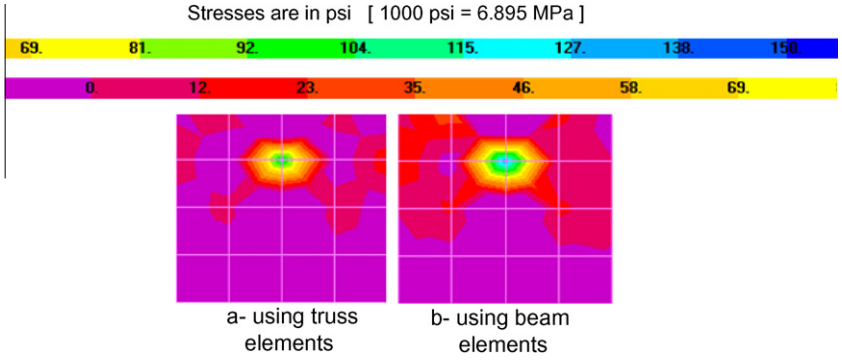

Fig. 14. Stress contours at the spliced bar cutoff point without transverse reinforcement in the splice region.

elements for beams without transverse reinforcement as shown in Fig. 14a and b.

6. Conclusions

Based on the experimental and the analytical studies, the following conclusions can be drawn:

1. Splitting failure of the concrete specimens reinforced with No. 20 (63.5 mm diameter) bars was sudden, violent and occurred along the entire length of the splice. It is recommended to use minimum transverse reinforcements within the splice region to confine the failure and to control propagation of splitting cracks.
2. The splice strength of No. 20 (63.5 mm diameter) bars is more influenced by the amount of transverse reinforcement used within the splice region compared to that of No. 9 (28 mm diameter) bars.
3. Regardless of the length used to splice No. 20 (63.5 mm diameter) bars, the bars will not develop its yield strength without the presence of transverse reinforcement within the splice region. Using a development length of 72 times the diameter of the bar developed only 80% of the yield strength of bars.
4. The ACI Committee 408 design expression predicted consistently higher stresses for the concrete beams reinforced with No. 20 (63.5 mm diameter) bars in comparison to the measured values. This trend was more pronounced for the confined specimens and could be attributed to the large relative rib area of these bars, which exceeded the values used in calibrating the ACI Committee 408 design expression.
5. The proposed expression by Orangun et al. [2] provides reasonable estimates of the splice strength for both regular- and large-diameter bars with or without transverse reinforcement confining the splice region.
6. Additional splitting stresses ranging from 15 to 25% can be induced as a result of accounting for the bars' moment of inertia and its tendency to straighten out as the beam deforms.
7. The ACI 318 Building Code provisions for bond and development can be extended to No. 20 (63.5 mm diameter) bars. However, to achieve a reasonable safety margin as that for regular bar diameters, it is recommended to increase the development length by 25% to account for additional splitting stresses developed by large diameter bars.

References

[1] ACI Committee 408. Bond and development of straight reinforcing in tension ACI 408R-03). Farmington Hills (MI): American Concrete Institute; 2003. p. 49.
[2] Orangun CO, Jirsa JO, Breen JE. Reevaluation of test data on development length and splices. ACI J Proc 1977;74(3):114–22.
[3] Darwin D, Tholen ML, Idun EK, Zuo J. Splice strength of high relative rib area reinforcing bars. ACI Struct J 1996;93(1):95–107.
[4] Darwin D, Zuo J, Tholen ML, Idun EK. Development length criteria for conventional and high relative rib area reinforcing bars. ACI Struct J 1996;93(3):347–59.
[5] Zuo J, Darwin D. Splice strength of conventional and high relative rib area bars in normal and high-strength concrete. ACI Struct J 2000;97(4):630–41.
[6] Untrauer RE. Discussion of development length for large high strength reinforcing bars. ACI J Proc 1965;62(9):1153–4.
[7] Tepfers R. A theory of bond applied to overlapping tensile reinforcement splices for deformed bars, publication 73:2, division of concrete structures. Goteborg, Sweden: Chalmers University of Technology; 1973. p. 328.
[8] Ferguson PM, Thompson JN. Development length for large high strength reinforcing bars. ACI J Proc 1965;62(1):71–94.
[9] Lutz LA, Gergely P. Mechanics of bond and slip of deformed bars in concrete. ACI J Proc 1967;64(11):711–21.
[10] Darwin D, Barham S, Kozul R, Luan S. Fracture energy of high-strength concrete. ACI Mater J 2001;98(5):410–7.
[11] ACI Committee 318. Building code requirements for structural concrete (ACI 318-08) and commentary (ACI 318R-08). Farmington Hills (MI): American Concrete Institute; 2008. p. 430.
[12] ASTM A 370-07. Standard test methods and definitions for mechanical testing of steel products. West Conshohocken, PA: ASTM International; 2007. p. 47.
[13] ANATECH Corp. ANATECH Concrete Analysis Program (ANACAP). Version 2.2.3 Reference Manuals; 2003.
[14] Rashid YR. Analysis of prestressed concrete pressure vessels. Nucl Eng Des 1968;7(4):334–44.
[15] Hassan T, Selim H, Rizkalla S, Zia P. Shear behavior of large-size concrete beams reinforced with high- and conventional-strength steel. ACI Struct J 2008;105(2):173–9.
[16] Hassan T, Lucier G, Rizkalla S, Zia P. Modeling of L-shaped, precast, prestressed concrete spandrels. PCI J 2007;52(2):78–92.
[17] Hassan T, Rizkalla S. Flexural strengthening of post-tensioned bridge slabs with FRP systems. PCI J 2002;47(1):76–93.
[18] Computers and Structures, Inc. SAP2000. Version 11.0. Berkeley (CA): Integrated Structural Analysis and Design Software; 2007.